

## Quantum-dot electron occupancy controlled by a charged scanning probe

R. Crook,<sup>1</sup> C. G. Smith,<sup>1</sup> W. R. Tribe,<sup>2</sup> S. J. O'Shea,<sup>3</sup> M. Y. Simmons,<sup>4</sup> and D. A. Ritchie<sup>1</sup>

<sup>1</sup>*Department of Physics, Cavendish Laboratory, Madingley Road, Cambridge CB3 0HE, United Kingdom*

<sup>2</sup>*TeraView Ltd., 302/304 Cambridge Science Park, Milton Road, Cambridge CB4 0WG, United Kingdom*

<sup>3</sup>*Institute of Materials Research and Engineering, 3 Research Link, Singapore 117602*

<sup>4</sup>*School of Physics, University of New South Wales, Sydney 2052, Australia*

(Received 14 May 2002; revised manuscript received 17 July 2002; published 3 September 2002)

A 1D channel, defined in a GaAs/AlGaAs heterostructure, has been used to detect the oscillations in charge as single electrons tunnel into or out of a group of quantum dots about  $1 \mu\text{m}$  from the channel. The quantum dots were formed in the highly doped donor layer of the same device due to intrinsic donor disorder. Electron occupancy of the quantum dots was controlled by the position and bias of a charged probe. High-resolution images of channel conductance revealed sets of concentric oscillations, or halos, each set being centered on a quantum dot. Uneven spacing was observed between the halos implying that the dot electron energy-level spacings were not constant. This is characteristic of a dot occupied by a small number of electrons. Changes in halo spacing at intersections between different sets of halos suggest that there was electrostatic interaction between the quantum dots.

DOI: 10.1103/PhysRevB.66.121301

PACS number(s): 73.23.Hk, 73.23.Ad, 73.20.Hb, 07.79.-v

The unique spacial information provided by scanning probe experiments promises to advance the understanding of electronic transport phenomena in the weakly disordered systems of real devices. Recent scanned gate microscopy experiments have observed single-electron charging in single-walled carbon nanotube quantum dots,<sup>1</sup> and interference effects in long quantum wires.<sup>2</sup> Fascinating images of back-scattered electron flux emanating from a one-dimensional (1D) channel have been presented over the last few years.<sup>3-7</sup> Such images are generated by recording the device conductance while a charged probe scans over either the nanotube or channel,<sup>1,2</sup> or the 2D electron reservoir adjacent to the channel.<sup>3-7</sup>

When the width of a 1D channel is adjusted so that a 1D subband<sup>8</sup> is partially transmissive, the channel conductance becomes extremely sensitive to changes in the local electrostatic potential. This sensitivity has been exploited by a number of experiments to detect the charge of a single electron.<sup>9-11</sup> In one such experiment, a 1D channel was fabricated adjacent to a quantum dot which was weakly coupled to two electron reservoirs.<sup>10</sup> As the dot was electrostatically squeezed by a plunger gate, each of the dot's energy levels came in range of the reservoir Fermi energy, making it energetically favorable to decrease the number of electrons in the dot by one. The resulting  $\pm e/2$  oscillations in the total charge of the quantum dot were observed as a sawtooth wave form in the conductance of the adjacent 1D channel.

This paper describes a recent experiment which also used a 1D channel to detect the single-electron charging of a quantum dot. The position and bias of a charged probe controlled the electron occupancy of several quantum dots. The quantum dots were formed in the donor layer adjacent to the channel due to donor fluctuations intrinsic to the device. The images revealed complex patterns of concentric circular oscillations, or halos, centered on the quantum dots, superimposed upon weak images of backscattered electron flux. Of particular interest are uneven spacing between halos, and the intersections between different sets of halos.

A high mobility 2D electron system (2DES) was formed  $77 \text{ nm}$  beneath the device surface at a GaAs/AlGaAs hetero-junction. After illumination with a red-light-emitting diode, the electron mobility was  $150 \text{ m}^2 \text{ V}^{-1} \text{ s}^{-1}$ , and the 2DES sheet density was  $4.6 \times 10^{15} \text{ m}^{-2}$ . The transport mean free path was calculated as  $16 \mu\text{m}$ , and the 2DES Fermi wavelength as  $37 \text{ nm}$ . Immediately after strong illumination, quantum Hall measurements indicated that part of the device donor layer was conducting in addition to the intended 2DES layer as illustrated in Fig. 1(a). Scanning in atomic force microscope (AFM) contact mode is known to locally reduce the 2DES electron density by raising  $E_c$  relative to  $E_F$ ,

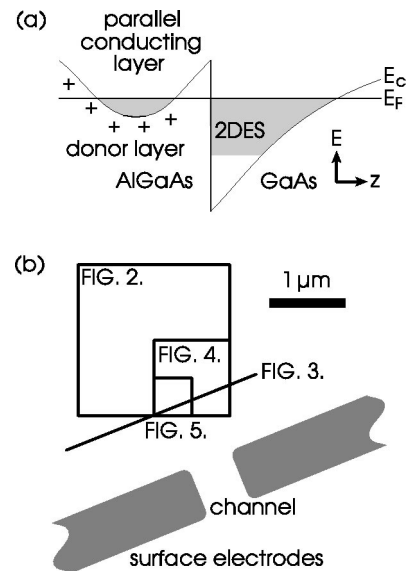


FIG. 1. (a) Conduction-band edge showing the formation of a parallel conducting layer. (b) Scale diagram showing the surface electrodes used to define the channel, and the areas scanned for subsequent figures.

thereby also reducing the density of transport electrons in the donor layer. The device was scanned repeatedly to raise  $E_c$  till the conducting donor layer broke up into electron puddles, or quantum dots, due to the inherent disorder of the charged donors. It was in this regime that the images presented in this paper were generated. Figure 1(b) shows a scale diagram of the surface electrodes used to define the channel and the areas scanned in subsequent figures. The split-gate surface electrodes were fabricated using electron-beam technology with a lithographic gate width and length of 500 nm. A negative bias was applied to the surface electrodes to deplete the underlying electrons and define a channel in the 2DES.

The charged probe was a modified AFM incorporating a conductive boron-doped silicon tip supported by a piezoresistive cantilever.<sup>12,13</sup> To locate a channel, the probe functions as an AFM making topographic images of the surface electrodes. To generate the conductance images and profiles presented in this paper the probe operates in a different mode. The charged probe was scanned 50 nm above the device surface while the channel conductance was recorded to determine the image or profile contrast. The channel conductance was measured by applying a 0.2-mV or 2-mV low-frequency ac signal across the channel and measuring the amplified channel ac current with a lock-in amplifier. A  $-4$ -V dc bias was applied to the tip. This bias is larger than a typical top-gate bias due to the tip's conical geometry and, because the tip does not touch the device surface, additional screening by surface states. Significant backscattering was not observed in these conductance images, which implies that the tip bias was not sufficiently negative to deplete electrons from the 2DES under the tip. Note that in other experiments reported elsewhere, with a tip bias of  $-8$  V, strong backscattering was observed in conductance images of the same device.<sup>14</sup> Data was taken at 20 mK in an Oxford Instruments Kelvinox dilution refrigerator.

Figure 2 presents a conductance image of the  $2 \mu\text{m} \times 2 \mu\text{m}$  area identified in Fig. 1(b). The image reveals a complex pattern including two clear sets of concentric halos. The halo centers are distinct and in this case are separated by about  $1 \mu\text{m}$ . Where the two sets of halos intersect, they superimpose, which implies that the mechanism responsible for this structure is located in the device. If the mechanism was located in the probe, which has a radius much less than the  $1 \mu\text{m}$  separation, then a pattern of contours without intersections would be observed on this spacial scale. Interference fringes originating from coherent backscattering have been reported in a similar experiment,<sup>6,7</sup> where the fringes were spaced close to  $\lambda_F/2$ . Here the spacing between halos is not constant, but is normally greater than 50 nm. In this device  $\lambda_F/2 = 18$  nm, so an interference origin for the halos is ruled out. The halos in Fig. 2 are not circular, but slightly elongated in the  $y$  direction. This distortion is thought to be due to scanning the cantilever at a slight angle to the device. Similar halo images have been generated by single-walled carbon nanotubes<sup>1</sup> and channels.<sup>9</sup> The halos were interpreted as tip controlled single-electron charging of quantum dots associated with defects.

Figure 3 presents two sets of conductance profiles along

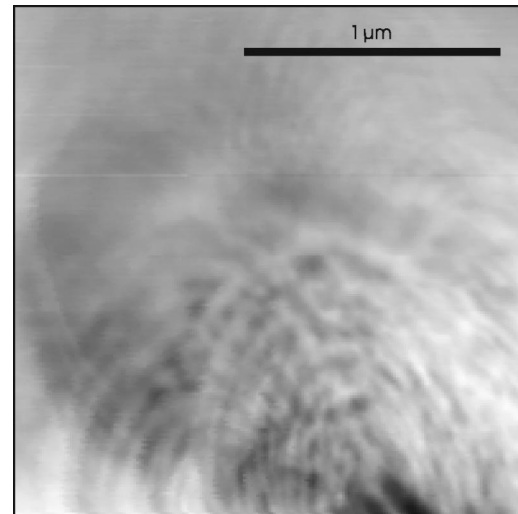


FIG. 2. Conductance image of the  $2 \mu\text{m} \times 2 \mu\text{m}$  area identified in Fig. 1(b), at 20 mK in 0 T with a 0.2-mV ac signal applied across the channel. Conductance varies from  $104 \mu\text{S}$  (black) to  $112 \mu\text{S}$  (white).

the line identified in Fig. 1(b) where the contrast is again set by the channel conductance. The  $x$  axis is the tip position along the line, and the  $y$  axis is either (a) the gate bias or (b) the tip bias. The fine structure in Fig. 3(a) is almost independent of the gate bias, but the broad structure is not. Conversely, the broad structure in Fig. 3(b) is independent of the tip bias, but the fine structure is not. Therefore, the mechanism responsible for the fine structure in the profiles, which corresponds to halos in the conductance images, does not originate in the channel. Instead, the channel is detecting changes in charge in the vicinity of the tip. However, the mechanism responsible for the broad structure in the profiles, which corresponds to broad changes in the background conductance in the images, does originate in the channel. The channel potential, and therefore the channel conductance, is modified by direct coupling from the channel to the scanning cantilever and tip.

The origin of the halos is further investigated in Fig. 4 where the channel bias and magnetic field are varied. Figure 4 presents conductance images of the  $1 \mu\text{m} \times 1 \mu\text{m}$  area identified in Fig. 1(b). Figures 4(a) and 4(b) were made with a 0.2-mV and 2-mV ac signal applied across the channel,

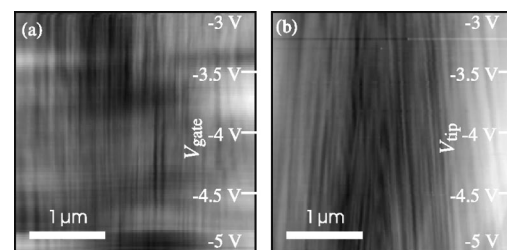


FIG. 3. Conductance profiles along the  $3\text{-}\mu\text{m}$  line identified in Fig. 1(b), as a function of (a) gate bias and (b) tip bias, at 20 mK in 0 T with a 0.2-mV ac signal applied across the channel. Each horizontal line is normalized. Conductance varies from (a)  $39 \mu\text{S}$  to  $112 \mu\text{S}$  and (b)  $76 \mu\text{S}$  to  $106 \mu\text{S}$ .

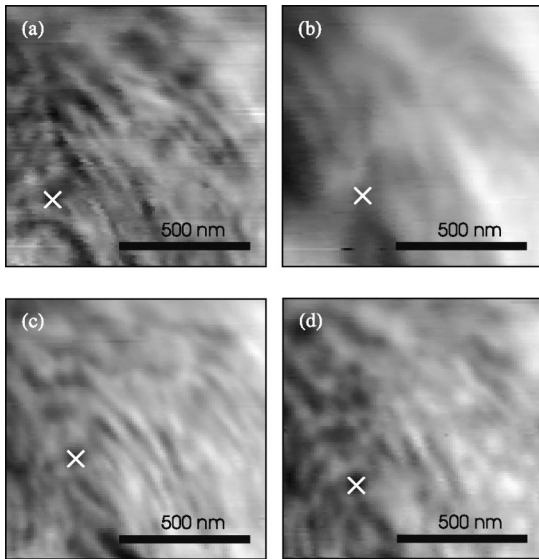


FIG. 4. Conductance images of the  $1 \mu\text{m} \times 1 \mu\text{m}$  area identified in Fig. 1(b), at 20 mK in (a) 0 T with 0.2 mV ac applied across the channel, (b) 0 T with 2 mV ac applied across the channel, (c) 10 mT with 0.2 mV ac applied across the channel, and (d) 50 mT with 0.2 mV ac applied across the channel. Conductance varies from  $\approx 105 \mu\text{S}$  to  $110 \mu\text{S}$  in all these images. The scanning probe drifted between images so the white cross identifies a common point.

respectively. With a 2-mV signal, the halo structure becomes blurred or broader but there is no reduction in the signal-to-noise ratio. This observation is not consistent with a reduction in channel sensitivity, which would occur with increased electron temperature. Instead, the increased voltage smears the energy distribution of transport electrons by up to 2 meV at the exit and entrance of the channel. This extended energy distribution persists several microns into the adjacent 2DES until the nonequilibrium electrons relax to the local Fermi level.<sup>4</sup> If the electrons tunneling into or out of the quantum dots originate in the 2DES, then they are also subject to the 2-meV smearing, and this explains the blurring seen in Fig. 4(b). Reducing the voltage across the channel below 0.2 mV ac did not reveal additional detail.

Figure 4(c) was generated in a 10 mT perpendicular magnetic field, whereas Fig. 4(d) was made in a 50 mT magnetic field. In 10 mT, the electron magnetic length  $(\hbar/eB)^{1/2}$  is 260 nm. Remote backscattered interference effects require an electron path length of at least twice the distance from the tip to the channel.<sup>6,7</sup> If the halo images were caused by interference around a closed path, then the structure would be radically changed in such a field. In 50 mT, the electron cyclotron radius is  $2 \mu\text{m}$ , which is sufficient to destroy any electron backscattering of more than a micron from the channel.<sup>4</sup> The images change very little in magnetic fields from 0 T to 50 mT, so neither interference nor backscattering are involved in the generation of these images. Note that these magnetic fields are too small to significantly modify the channel conductance characteristics.

From this gallery of images, it is possible to understand the origin of the halos. The channel is behaving like a local

electrometer, measuring the total potential from a number of quantum dots formed in the donor layer near the channel. The quantum dots are weakly coupled to the 2DES. Quantum dots which are either strongly coupled to or isolated from the 2DES may exist but are not observed. As the charged tip approaches a quantum dot, the dot electrostatic potential increases until it becomes energetically favorable for an electron to tunnel out of the quantum dot into the 2DES. As the tip moves towards the center of the dot, further electrons tunnel out, causing oscillations in the dot potential. These oscillations are observed in conductance images as a set of concentric halos centered over the dot. Different sets of halos are associated with different quantum dots, so the halos superimpose when they intersect.

The charge induced on the dot is equal to  $V_{\text{tip}}C(\rho, d)$ , where  $C$  is the capacitance between the dot and the tip,  $\rho$  is the in-plane distance from tip to dot, and  $d$  is the tip to 2DES separation incorporating changes in permittivity. Adjacent halos correspond to a one electron charge  $e$  change in the charge of the quantum dot, so  $V_{\text{tip}}\Delta\rho\partial C/\partial\rho = e$ , where  $\Delta\rho$  is the halo spacing. If the tip electric field is assumed to be that of a point charge, then  $C = 4\pi\epsilon k[r_{\text{tip}}^{-1} - (\rho^2 + d^2)^{-0.5}]^{-1}$ , where  $r_{\text{tip}}$  is the tip radius and  $k$  is an unknown constant to incorporate screening effects. Therefore, in the limit  $r_{\text{tip}} \ll (\rho^2 + d^2)^{0.5}$ , the halo spacing is proportional to

$$(V_{\text{tip}}\rho)^{-1}(\rho^2 + d^2)^{1.5}. \quad (1)$$

Moving away from the dot, where  $\rho \gg d$ , the halo spacing increases, becoming proportional to  $\rho^2$ . Near the center of the dot the halo spacing also increases although an abrupt absence of halos may indicate that the dot has been completely emptied of electrons. Both these predictions are evident in Fig. 2. As the tip bias is taken more negative the halos migrate away from the center moving closer together as new halos appear at the center. This is seen moving down the profiles shown in Fig. 3(b).

The conductance amplitude of the halo oscillations depends upon the the channel to dot capacitance, which is equal to  $e/\Delta V$ , where  $\Delta V$  is the potential oscillation at the channel. With reference to a previous experiment using a channel with similar physical and electrical characteristics,<sup>9</sup> the ratio between channel electrostatic potential and conductance is  $\approx 30 \text{ V S}^{-1}$ . Measuring the strongest set of halos in Fig. 2, which are centered at  $1 \mu\text{m}$  from the channel, the channel to dot capacitance is  $\approx 0.7 \text{ fF}$ . The tip to dot capacitance can be deduced from Fig. 3(b). A profile in the  $V_{\text{tip}}$  direction reveals single-electron oscillations with a period between 0.5 V and 3 V depending upon how far the tip is from the dot. When the tip is close to a dot, the tip to dot capacitance is  $\approx e/(0.5 \text{ V}) = 0.3 \text{ aF}$ .

The large difference between the channel to dot and tip to dot capacitances is due to the strong 2DES coupling between the channel and the dot, and the effective surface-state screening between the tip and the dot. Figure 3 shows that the gate bias has little influence on the dot electron occupancy compared to the tip bias. It is thought that a decrease in gate bias raises both the dot and 2DES potential equally, because the dot is coupled to the gate via the 2DES. The tip

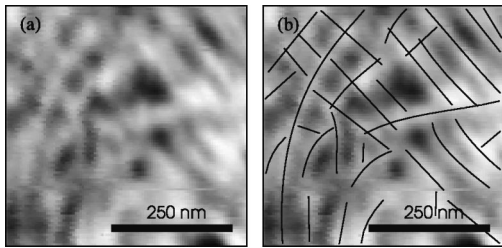


FIG. 5. (a) Conductance image of the  $500\text{ nm}\times 500\text{ nm}$  area identified in Fig. 1(b), at 20 mK in 0 T with 0.2 mV ac applied across the channel. Conductance varies from  $104\ \mu\text{S}$  to  $112\ \mu\text{S}$ . (b) The same image as (a) with lines added to trace the halos.

electric field at the dot is perpendicular to the 2DES, so a decrease in tip bias raises the dot potential more than the 2DES potential, and single-electron charging effects are observed.

Figure 5(a) presents a conductance image of the  $500\text{ nm}\times 500\text{ nm}$  area identified in Fig. 1(b). This image is presented to show that upon close inspection the patterns are far from being regular intersecting sets of halos. The same image is presented in Fig. 5(b) with lines added to trace the halos. Uneven spacing between halos is apparent in the im-

age, being particularly clear in the top right corner, where a double-single-double pattern is seen. This corresponds to uneven energy-level spacings, which is characteristic of quantum dots containing a small number of electrons.<sup>15</sup> At several places in the image there is strong evidence that the halo spacing changes at intersections between sets of halos. This suggests that there are electrostatic interaction effects between the quantum dots, where the electron occupancy of a quantum dot modifies the electron energy levels of a neighboring dot.

In conclusion, we have shown that a 1D channel can detect the oscillations in charge as single electrons tunnel into or out of a group of quantum dots. The quantum dot electron occupancy was controlled by the position and bias of a scanning charged probe. High-resolution images revealed sets of concentric oscillations, each set being centered on a quantum dot, and each oscillation corresponding to the addition of a single electron. When a dot is occupied by a small number of electrons, the energy-level spacings are not constant, which was observed as uneven spacing between oscillations. Changes in oscillation spacing at intersections suggests an electrostatic interaction between the quantum dots.

This work was supported by the UK EPSRC.

<sup>1</sup>M.T. Woodside and P.L. McEuen, *Science* **296**, 1098 (2002).

<sup>2</sup>T. Ihn, J. Rychen, T. Cilento, R. Held, K. Ensslin, W. Wegscheider, and M. Bichler, *Physica E (Amsterdam)* **12**, 691 (2002).

<sup>3</sup>M.A. Eriksson, R.G. Beck, M. Topinka, J.A. Katine, R.M. Westervelt, K.L. Campman, and A.C. Gossard, *Appl. Phys. Lett.* **69**, 671 (1996).

<sup>4</sup>R. Crook, C.G. Smith, C.H.W. Barnes, M.Y. Simmons, and D.A. Ritchie, *J. Phys.: Condens. Matter* **12**, L167 (2000).

<sup>5</sup>R. Crook, C.G. Smith, M.Y. Simmons, and D.A. Ritchie, *Phys. Rev. B* **62**, 5174 (2000).

<sup>6</sup>M.A. Topinka, B.J. LeRoy, S.E.J. Shaw, E.J. Heller, R.M. Westervelt, K.D. Maranowski, and A.C. Gossard, *Science* **289**, 2323 (2000).

<sup>7</sup>M.A. Topinka, B.J. LeRoy, R.M. Westervelt, S.E.J. Shaw, R. Fleischmann, E.J. Heller, K.D. Maranowski, and A.C. Gossard, *Nature (London)* **410**, 183 (2001).

<sup>8</sup>R. Landauer, *IBM J. Res. Dev.* **1**, 223 (1957).

<sup>9</sup>R. Crook, C.G. Smith, M.Y. Simmons, and D.A. Ritchie, *J. Phys.: Condens. Matter* **13**, L249 (2001).

<sup>10</sup>M. Field, C.G. Smith, M. Pepper, D.A. Ritchie, J.E.F. Frost, G.A.C. Jones, and D.G. Hasko, *Phys. Rev. Lett.* **70**, 1311 (1993).

<sup>11</sup>D.H. Cobden, A. Savchenko, M. Pepper, N.K. Patel, D.A. Ritchie, J.E.F. Frost, and G.A.C. Jones, *Phys. Rev. Lett.* **69**, 502 (1992).

<sup>12</sup>M. Tortonese, R.C. Barret, and C.F. Quate, *Appl. Phys. Lett.* **62**, 834 (1993).

<sup>13</sup>ThermoMicroscopes, Sunnyvale, CA.

<sup>14</sup>R. Crook, C. G. Smith, W. R. Tribe, M. Y. Simmons, and D. A. Ritchie, in *Proceedings of the 26th International Conference on the Physics of Semiconductors, Edinburgh, 2002*, edited by Andrew R. Long and John H. Davies (IOP, London, in press).

<sup>15</sup>P.L. McEuen, *Science* **278**, 1729 (1997).